The North Atlantic Ocean Is in a State of Reduced Overturning

D. A. Smeed[1] , S. A. Josey[1], C. Beaulieu[2] , W. E. Johns[3], B. I. Moat[1] , E. Frajka-Williams[2] , D. Rayner[1] , C. S. Meinen[4] , M. O. Baringer[4] , H. L. Bryden[2] , and G. D. McCarthy[1,5]

[1]National Oceanography Centre, Southampton, UK, [2]Ocean and Earth Science, University of Southampton, Southampton, UK, [3]Rosenstiel School of Marine and Atmospheric Science, University of Miami, Miami, FL, USA, [4]Atlantic Oceanographic and Meteorological Laboratory, NOAA, Miami, FL, USA, [5]ICARUS, Department of Geography, Maynooth University, Maynooth, Ireland

Abstract The Atlantic Meridional Overturning Circulation (AMOC) is responsible for a variable and climatically important northward transport of heat. Using data from an array of instruments that span the Atlantic at 26°N, we show that the AMOC has been in a state of reduced overturning since 2008 as compared to 2004–2008. This change of AMOC state is concurrent with other changes in the North Atlantic such as a northward shift and broadening of the Gulf Stream and altered patterns of heat content and sea surface temperature. These changes resemble the response to a declining AMOC predicted by coupled climate models. Concurrent changes in air-sea fluxes close to the western boundary reveal that the changes in ocean heat transport and sea surface temperature have altered the pattern of ocean-atmosphere heat exchange over the North Atlantic. These results provide strong observational evidence that the AMOC is a major factor in decadal-scale variability of North Atlantic climate.

1. Introduction

The Atlantic Meridional Overturning Circulation (AMOC) transports warm near-surface waters northward and colder deep waters southward, resulting in a large transport of heat. In model studies, the AMOC plays a major role in climate variability not only around the North Atlantic and peripheral land masses but globally (Buckley & Marshall, 2016). Climate models predict that under the influence of anthropogenic warming, the AMOC will decline during this century at a rate between 0 and 0.9 Sv per decade (Intergovernmental Panel on Climate Change, 2013) (1 Sv = 10^6 m^3 s^{-1}), and more extreme scenarios have been proposed (Hansen et al., 2016; Liu et al., 2017). Thus, understanding the rate of change of the AMOC in the real ocean is a matter of major importance (Rahmstorf et al., 2015).

Analysis of internal or forced variability of the climate system over decade-to-century time scales is primarily accomplished using coupled ocean-ice-atmosphere models. This is because in situ subsurface ocean observation records with sufficient accuracy to quantify decadal changes have not been available throughout most of the oceans. Only since the commencement of continuous observation of the AMOC in 2004 by the RAPID/Meridional Overturning Circulation and Heatflux Array/Western Boundary Time Series array at 26°N (hereafter the RAPID 26°N array) has it been possible to accurately quantify the temporal variability of the AMOC (Smeed et al., 2014). A number of studies have suggested that much of the interannual variability of the AMOC has been forced by atmospheric wind stress changes (Polo et al., 2014; Zhao & Johns, 2014a, 2014b). On longer time scales, climate simulations suggest that there are cycles of air-sea interaction in which reduced heat loss from the ocean to the atmosphere over the subpolar gyre results in less deepwater formation, thus slowing the lower limb of the overturning circulation (Roberts et al., 2013). The diminished ocean meridional heat transport leads to a reduction in subpolar gyre heat content until eventually heat loss over deepwater formation regions, such as the Labrador and Irminger Seas, increases again, reinvigorating the overturning circulation. A decline in the density of water in the Labrador Sea since the late 1990s has led to the hypothesis that a reduction of the AMOC after 2008 is part of such a cycle (Robson et al., 2013). However, variability in freshwater transport is also important in controlling density in the subpolar gyre and significant variability in mechanisms has been found in model studies (see, e.g., Buckley & Marshall, 2016; Roberts et al., 2013).

Previous observations of the AMOC found a 0.6 Sv year^{-1} decrease over the period from 2007 to 2011 (Smeed et al., 2014). This is an order of magnitude larger than the long-term forced trend predicted by Coupled Model Intercomparison Project Phase 5 coupled models (Intergovernmental Panel on Climate

Change, 2013), and Smeed et al., (2014) concluded the observed changes were most likely caused by decadal change rather than a long-term decline. A part of the change may be forced by anthropogenic warming, but the observational record is not yet long enough to separate long-term forced changes from decadal-scale internal variability. Using new observations at 26°N (Smeed et al., 2017), we show that the AMOC has not reduced further during 2012–2017 but has continued to occupy a weaker circulation state relative to the first years of observations. In the following sections, we show that this change of AMOC state is concurrent with other changes in the North Atlantic such as a northward shift and broadening of the Gulf Stream, evidenced by a change in the currents observed by satellite altimetry and by an altered pattern of sea surface temperature (SST). The observed change in heat content is described by a pattern that resembles the response to a declining AMOC predicted by coupled climate models (Tulloch & Marshall, 2012; Zhang, 2008). Concurrent changes in air-sea fluxes reveal that the changes in ocean heat transport and SST have altered the pattern of ocean-atmosphere heat exchange over the North Atlantic. These results provide strong observational evidence that the AMOC is a major factor in decadal-scale variability of North Atlantic climate.

2. The RAPID 26°N Array

There are four contributions to the calculation of the AMOC at 26°N (Figure S1 in the supporting information). The flow through the Florida Straits is monitored by a submarine cable calibrated by regular hydrographic measurements. The flow east of the Bahamas is monitored by an array of current meters that extend out 22 km offshore (location WB2) where the water depth is almost 4,000 m deep; east of this location, an array of temperature and salinity instruments span the Atlantic and the flow is calculated using geostrophic balance. The ageostrophic flow of the Ekman boundary layer is calculated from wind stress estimates from the ERA-Interim reanalysis product. A full description of the methodology is given by McCarthy et al. (2015). These data allow the annual mean values of the AMOC to be estimated with an accuracy of about 0.9 Sv. For comparison annual-mean values during 2004–2016 have a standard deviation of 1.9 Sv and a range of 7.3 Sv (see Table S1).

The time series of the vertical profile of the overturning transport is also calculated from the data. From this the transports associated with the upper and lower North Atlantic Deep Waters (NADW) are derived. The transport of lower NADW is estimated as the transport between 3,000 m and 5,000 m depth, and the transport of upper NADW is estimated as the transport between 1,100 m and 3,000 m depth.

We estimate the transport of the Antilles Current by integrating the northward flow above 1,100 m measured by the current meter array out to location WB2. This transport is added to that through Florida Straits to obtain a total western boundary current (WBC) transport. The gyre recirculation is then calculated as the total AMOC less the WBC transport, and less the Ekman transport.

3. Analysis of the 26°N Time Series

The time series of the AMOC at 26°N spans April 2004 to February 2017 and is thus now 13 years long (Figure 1). It shows high values for the AMOC prior to 2008, followed by a decline and a relatively constant strength thereafter. The downturn in 2009–2010 (McCarthy et al., 2012) is also evident. To formally examine whether or not the reduction of the AMOC has continued over the 5 years since the decline was first reported, we have used change-point analysis (Beaulieu et al., 2012). For this analysis, we used de-seasonalized monthly mean values of the RAPID 26°N time series. The model that best represents the data is consistent with two periods of relatively constant AMOC with a rapid change occurring in 2008. When compared with the null hypothesis that there is no change-point, the change is significant at the 99% level for both the total AMOC and the AMOC less the Ekman transport. Excluding data from the time of the extreme reduction in 2008–2009 has only a small impact on the results (Table S2).

We have also compared the mean value for three time periods: the two four-year periods used in the previous study (Smeed et al., 2014) (2004–2008 and 2008–2012) and the five-year period from 2012 to 2017 (Table S3). Prior to April 2008, the AMOC had a mean value of 18.8 Sv; in the following two periods, the mean values were 15.9 and 16.3 Sv. The first reduction of 2.9 Sv is significant at the 95% level, but the subsequent increase of 0.4 Sv is not.
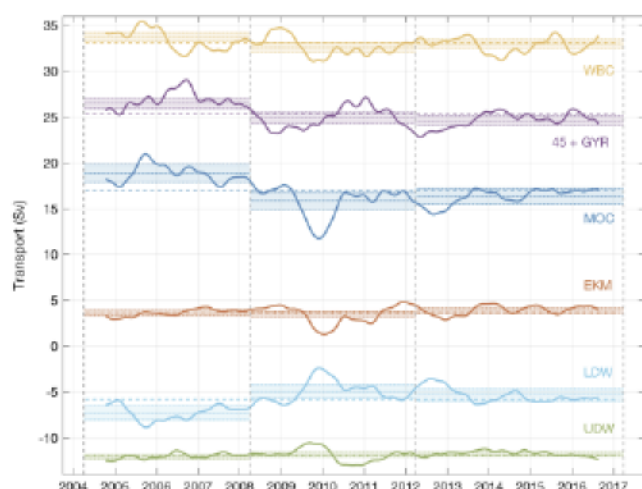
Figure 1. Low-pass filtered transports from 26°N. For all variables, positive values imply northward transport. The total Atlantic Meridional Overturning Circulation (AMOC) (MOC) and the Ekman component (EKM) are shown. The non-Ekman part of the upper limb of the AMOC is the net sum of a northward western boundary component (WBC) and a southward recirculation in the gyre (GYR). So that it can be shown easily on the same plot, a value of 45 Sv has been added to GYR. The southward flowing lower limb of the AMOC is separated into the upper North Atlantic Deep Waters between 1,100 m and 3,000 m depth (UDW) and lower North Atlantic Deep Waters between 3,000 m and 5,000 m (LDW). The thick continuous lines are 12 month low-pass (Tukey) filtered data. The mean values for the whole time series are shown as dashed lines. Means are shown for three periods: April 2004 to March 2008, April 2008 to March 2012, and April 2012 to March 2017. The 95% confidence intervals for these means are shown by shading.

The slight increase in the AMOC since 2012 is primarily in the directly wind-driven Ekman component (Figure 1), but the changes in the Ekman driven overturning between the different time periods are not statistically significant (Table S3). In contrast, the change in the non-Ekman part of the circulation between 2004–2008 and 2008–2012 is significant. The non-Ekman component of the upper limb of the AMOC can be considered as the difference between northward flow of water in the WBCs and the southward recirculation of the subtropical gyre. The RAPID 26°N array observations enable us to estimate the contributions of these terms separately as described above (Figure 1). We find that 25% to 40% (depending upon which time period is considered) of the reduction in the non-Ekman part AMOC is due to a decrease in the northward flow of WBCs and 60% to 75% is due to an increase in the southern flow in the recirculation. The net northward flow in the upper limb of the AMOC is balanced by an equal and opposite southward flow below the thermocline, primarily in the deep WBC. Our results show that the reduction in northward flow of waters in the upper 1,000 m is balanced almost entirely by a reduction in the southward flow below 3,000 m. During the last 9 years, the transport of lower NADW has been about 30% less than during the first 4 years of measurements. In contrast, there has been no detectable long-term change in the transport of upper NADW.

4. Concurrent Changes in the North Atlantic

We have determined the extent to which other key climate parameters, heat content, sea surface height (SSH), SST, and air-sea latent heat flux (LHF, the dominant term in the net surface heat exchange) have varied concurrently with the AMOC state change by calculating the difference in their mean values for April 2004 to March 2008 and April 2008 to March 2017. In each case we have averaged an integer number of years, so that the results are not aliased by seasonal changes, and we focus on areas where the difference is significant at the 95% confidence level. Identifying concurrent changes is not sufficient to determine cause and effect, and the changes are likely influenced by processes other than the AMOC too, but the observed patterns show a strong resemblance to those predicted by models to occur in response to a changing AMOC (Zhang, 2008), indicating that they are consistent with a likely response to a reduced AMOC.

First, we consider heat content (Figure 3, top). These data are derived from the EN4 data set (Good et al., 2013) and are expressed as the average temperature in the upper 1,000 m. Figure 3 shows four areas of significant change: a warming off the east coast of North America between 40 and 45°N, a cooling in the eastern subpolar gyre south-east of Greenland, warming between 20°N and 30°N in the eastern subtropical gyre, and a small area of cooling to the southeastern edge of the Gulf Stream (near 40°N, 50°W). This resembles the pattern of subsurface temperature anomalies associated with a weakening AMOC found by Zhang (2008) (see Figure 2d in that paper showing temperature at 400 m depth, but note that the signs are reversed as the case of an increasing AMOC is considered). A similar modeled response to a changing AMOC is described by Tulloch and Marshall (2012). There are some differences between the observations presented here and the responses found in the modeling studies; in particular, relative to the model results, the anomalies in the Gulf stream region are displaced to the west in the observations. Another difference is that the observed warming in the eastern subtropics is stronger in the observations than in the model data. The range of mean temperature change in the upper 1,000 m in the modeling studies is similar, but a little larger, than that in our data. The range of subsurface temperature change presented by Tulloch and Marshall (2012) is roughly ±0.5 °C per Sv of AMOC change at 26°N (see their Figures 1f and 2e), whereas the corresponding value from our data is about ±0.3 °C Sv^{-1}.

Warming north of the Gulf Steam is also evident in the SST (Figure 2, fourth row, data from the Hadley Centre SST data set data set; Rayner et al., 2003) as is a rise in SSH (Figure 2, second row). Most of the change in SSH is
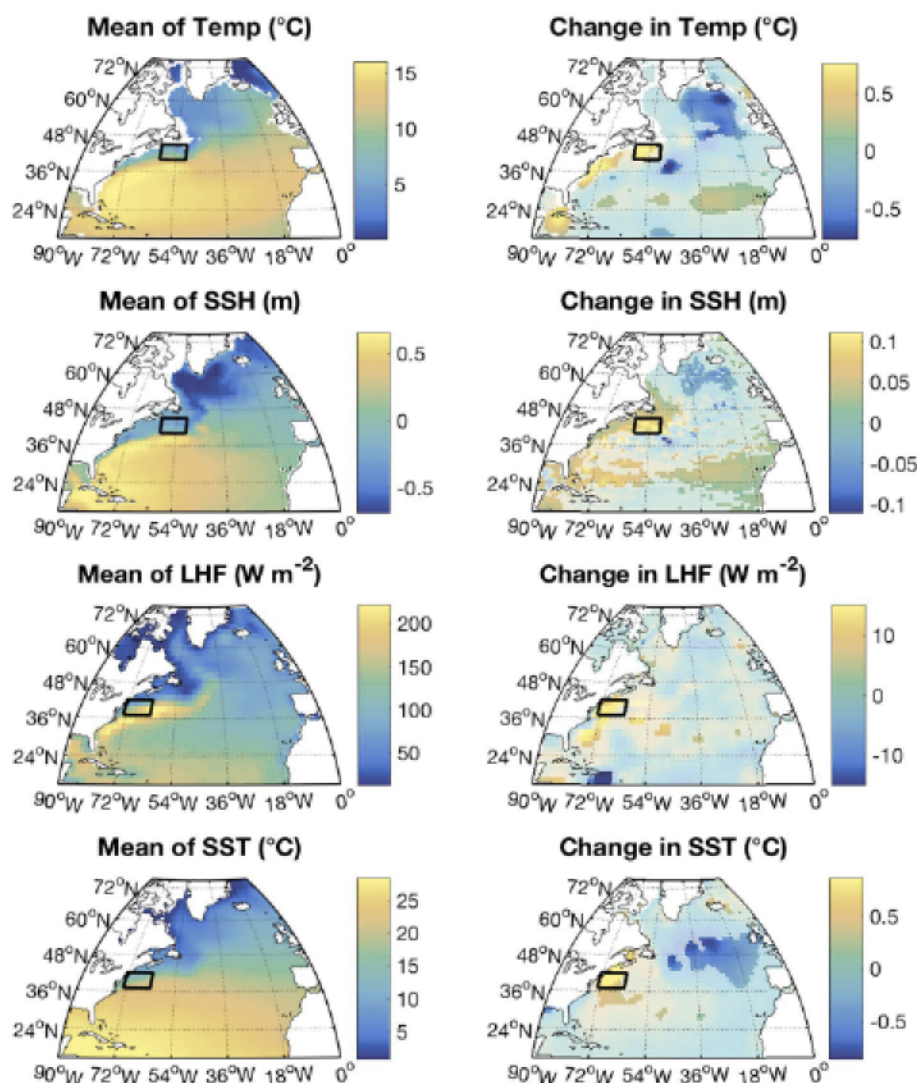
Figure 2. The left-hand column shows the mean fields of average temperature in the upper 1,000 m, sea surface height (SSH), latent heat flux (LHF), and sea surface temperature (SST); each is averaged over the period from 2004 to 2016. The changes in these variables are calculated as the mean over 2009 to 2016 less the mean from 2004 to 2008 and are shown in the right-hand column. The color is intensified where the change is significant at the 95% confidence level. The rectangles indicate the areas used to construct the indices plotted in Figure 3.

accounted for by steric height changes in the upper 1,000 m (Figure S2), indicating that the change in circulation is primarily in the waters within and above the main thermocline. While it is tempting to infer a broad northward shift in the Gulf Stream from these data, a closer look at the SSH (Figure S3) indicates that while the Gulf Stream is displaced northward west of about 60°W, east of this longitude, a broadening is evident. The high SSH in the eastern subtropics and the low SSH in the eastern subpolar latitudes suggest a strengthened eastward flow and recirculation in both the subtropical and subpolar gyres. There is also a reduction in the SSH gradient across 45°N, suggesting a reduced northward flow in the North Atlantic Current. These inferred circulation changes all suggest a reduced northward heat transport into the subpolar gyre. The pattern of SSH change has some resemblance to the second empirical orthogonal function of detrended SSH variability found by Foukal and Lozier (2017, their Figure 8), but the empirical orthogonal function does not have the high values in the eastern subtropics seen in our analysis.

Changes in ocean heat transport and SST are expected to modify the net air-sea heat flux. The changes in the total air-sea flux (Figure S4, data obtained from the National Centers for Environmental Prediction-National Center for Atmospheric Research reanalysis; Kalnay et al., 1996) are almost all due to the change in LHF. The third panel of Figure 3 shows the changes in LHF between the two periods. There is a strong signal
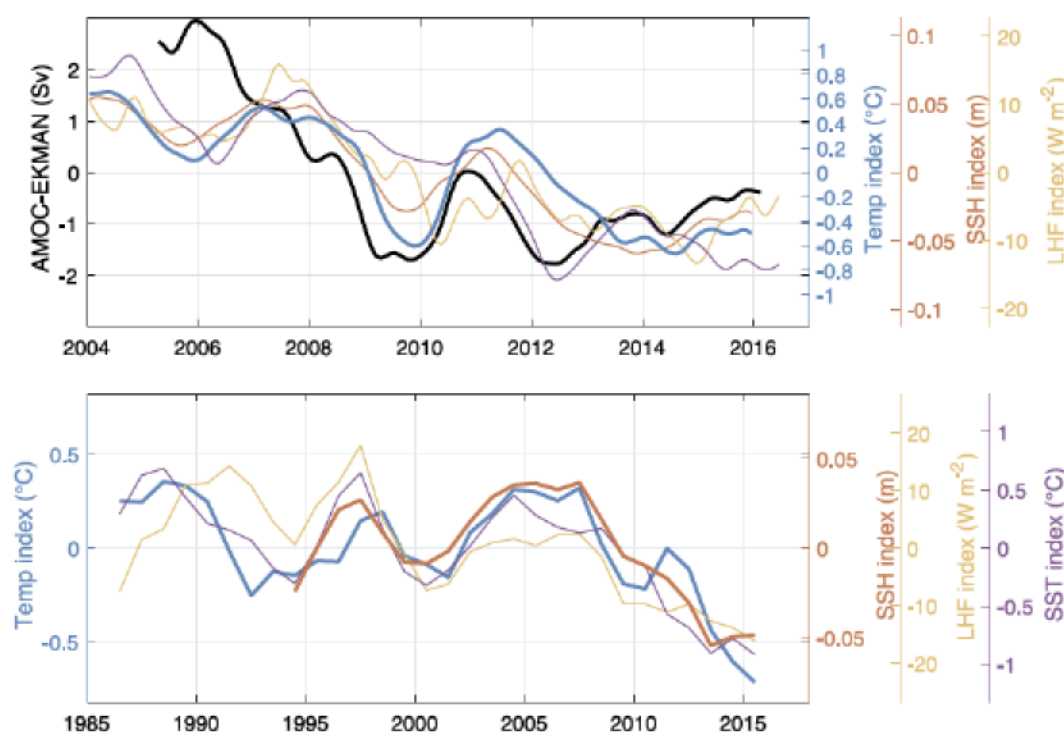
Figure 3. Indices of subsurface temperature, sea surface height (SSH), latent heat flux (LHF), and sea surface temperature (SST). SST (purple) is plotted using the same scale as subsurface temperature (blue) in the upper panel. The upper panel shows 24 month filtered values of de-seasonalized anomalies along with the non-Ekman part of the AMOC. In the lower panel, we show three-year running means of the indices going back to 1985 (1993 for the SSH index).

with increased heat loss from the ocean over the Gulf Stream. That the area of increased heat loss coincides with the location of warming SST indicates that the changes in air-sea fluxes are driven by the ocean.

5. Discussion

A number of studies with coupled climate models and forced ocean models have found that decadal-scale reductions in the AMOC are manifest by a weakening of the northward WBC (e.g., Thomas et al., 2012) and a reduction of the heat transported by the North Atlantic Current into the eastern subpolar gyre (Zhang, 2008). These are very similar to the changes that we have identified as concurrent with the observed reduction in the AMOC. The fingerprint of a changing AMOC in model simulations is usually determined by regressing the different variables against the AMOC. This approach has previously been applied to observations and revealed correlations between SST and the AMOC at 26°N associated with seasonal to interannual variability (Duchez et al., 2015). But, for the multiyear decline of the AMOC, the observational record is not sufficiently long to apply the same methodology and a different approach is needed.

To examine the temporal pattern of the changes, we have constructed indices for subsurface temperature, SSH, SST, and LHF. Each index is constructed by averaging the variable over the area of maximum change identified in Figure 2, and over the whole region from 15°N to 75°N, and then taking the difference between the two (see Figure 2. and Table S4 for area definitions). Taking the difference in this way allows us to separate changes in patterns from trends affecting the whole of the North Atlantic. Although these data alone are not sufficient to quantify lags between the different data sets, the results (Figure 3) show that the SSH, heat content, and LHF indices all change most rapidly between 2008 to 2010.

Whilst the AMOC has only been continuously measured since 2004, the indices of SSH, heat content, SST, and LHF can be calculated farther back in time (Figure 3, bottom). Over this longer time period, all four indices are strongly correlated with one another (Table S5; correlations were calculated using the nonparametric method described in McCarthy et al., 2015). These data suggest that measurement of the AMOC at 26°N started close to a maximum in the overturning. Prior to 2007 the indices show variability on a time scale of 8 to 10 years and no trend is evident, but since 2014 all indices have had values lower than any other year since 1985.

Model studies suggest that changes in the subpolar gyre precede changes in the subtropical AMOC by about 6 years, but that changes in the AMOC are almost coherent over latitudes from 25°N to 45°N (Jackson et al., 2016). Similar time scales have been deduced from observation of the deep WBCs (Le Bras et al., 2017; van Sebille et al., 2011). These time scales are consistent with a maxima of subpolar densities in the late 1990s (Yashayaev & Loder, 2016) before a mid-2000 peak in Atlantic overturning.

Previous studies have shown that seasonal and interannual changes in the subtropical AMOC are forced primarily by changing wind stress mediated by Rossby waves (Zhao & Johns, 2014a, 2014b). There is growing evidence (Delworth et al., 2016; Jackson et al., 2016) that the longer-term changes of the AMOC over the last decade are also associated with thermohaline forcing and that the changed circulation alters the pattern of ocean-atmosphere heat exchange (Gulev et al., 2013). The role of ocean circulation in decadal climate variability has been challenged in recent years with authors suggesting that external, atmospheric-driven changes could produce the observed variability in Atlantic SSTs (Clement et al., 2015). However, the direct observation of a weakened AMOC supports a role for ocean circulation in decadal Atlantic climate variability.

Our results show that the previously reported decline of the AMOC (Smeed et al., 2014) has been arrested, but the length of the observational record of the AMOC is still short relative to the time scales of important decadal variations that exist in the Atlantic. Understanding is therefore constantly evolving. What we identify as a changed state of the AMOC in this study may well prove to be part of a decadal oscillation superposed on a multidecadal cycle. Overlaying these oscillations is the impact of anthropogenic change that is predicted to weaken the AMOC over the next century. The continuation of measurements from the RAPID 26°N array and similar observations elsewhere in the Atlantic (Lozier et al., 2017; Meinen et al., 2013) will enable us to unravel and reveal the role of ocean circulation in the changing Atlantic climate in the coming decades.

References

Beaulieu, C., Chen, J., & Sarmiento, J. L. (2012). Change-point analysis as a tool to detect abrupt climate variations. *Philosophical Transactions of the Royal Society A: Mathematical, Physical and Engineering Sciences, 370*(1962), 1228–1249. https://doi.org/10.1098/rsta.2011.0383

Buckley, M. W., & Marshall, J. (2016). Observations, inferences, and mechanisms of the Atlantic Meridional Overturning Circulation: A review. *Reviews of Geophysics, 54*, 5–63. https://doi.org/10.1002/2015RG000493

Clement, A., Bellomo, K., Murphy, L. N., Cane, M. A., Mauritsen, T., Rädel, G., & Stevens, B. (2015). The Atlantic Multidecadal Oscillation without a role for ocean circulation. *Science, 350*(6258), 320–324. https://doi.org/10.1126/science.aab3980

Delworth, T. L., Zeng, F., Vecchi, G. A., Yang, X., Zhang, L., & Zhang, R. (2016). The North Atlantic Oscillation as a driver of rapid climate change in the Northern Hemisphere. *Nature Geoscience, 9*(7), 509–512. https://doi.org/10.1038/ngeo2738

Duchez, A., Courtois, P., Harris, E., Josey, S. A., Kanzow, T., Marsh, R., et al. (2015). Potential for seasonal prediction of Atlantic sea surface temperatures using the RAPID array at 26°N. *Climate Dynamics, 46*(9-10), 3351–3370. https://doi.org/10.1007/s00382-015-2918-1

Foukal, N. P., & Lozier, M. S. (2017). Assessing variability in the size and strength of the North Atlantic subpolar gyre. *Journal of Geophysical Research: Oceans, 122*, 6295–6308. https://doi.org/10.1002/2017JC012798

Good, S. A., Martin, M. J., & Rayner, N. A. (2013). EN4: Quality controlled ocean temperature and salinity profiles and monthly objective analyses with uncertainty estimates. *Journal of Geophysical Research: Oceans, 118*, 6704–6716. https://doi.org/10.1002/2013JC009067

Gulev, S. K., Latif, M., Keenlyside, N., Park, W., & Koltermann, K. P. (2013). North Atlantic Ocean control on surface heat flux on multidecadal timescales. *Nature, 499*(7459), 464–467. https://doi.org/10.1038/nature12268

Hansen, J., Sato, M., Hearty, P., Ruedy, R., Kelley, M., Masson-Delmotte, V., et al. (2016). Ice melt, sea level rise and superstorms: Evidence from paleoclimate data, climate modeling, and modern observations that 2 °C global warming could be dangerous. *Atmospheric Chemistry and Physics, 16*(6), 3761–3812. https://doi.org/10.5194/acp-16-3761-2016

Intergovernmental Panel on Climate Change (2013). In T. F. Stocker, et al. (Eds.), *Climate change 2013: The physical science basis. Contribution of Working Group I to the Fifth Assessment Report of the Intergovernmental Panel on Climate Change* (p. 1535). Cambridge, United Kingdom and New York: Cambridge University Press.

Jackson, L. C., Peterson, K. A., Roberts, C. D., & Wood, R. A. (2016). Recent slowing of Atlantic overturning circulation as a recovery from earlier strengthening. *Nature Geoscience, 9*(7), 518–522. https://doi.org/10.1038/ngeo2715

Kalnay, E., Kanamitsu, M., Kistler, R., Collins, W., Deaven, D., Gandin, L., et al. (1996). The NCEP/NCAR 40-Year Reanalysis Project. *Bulletin of the American Meteorological Society, 77*(3), 437–471. https://doi.org/10.1175/1520-0477(1996)077%3C0437:TNYRP%3E2.0.CO;2

Le Bras, I. A., Yashayaev, I., & Toole, J. (2017). Tracking Labrador Sea water property signals along the deep western boundary current. *Journal of Geophysical Research: Oceans, 122*, 5348–5366. https://doi.org/10.1002/2017JC012921

Liu, W., Xie, S.-P., Liu, Z., & Zhu, J. (2017). Overlooked possibility of a collapsed Atlantic Meridional Overturning Circulation in warming climate. *Science Advances, 3*(1), e1601666. https://doi.org/10.1126/sciadv.1601666

Lozier, S. M., Bacon, S., Bower, A. S., Cunningham, S. A., Femke de Jong, M., de Steur, L., et al. (2017). Overturning in the Subpolar North Atlantic Program: A new international ocean observing system. *Bulletin of the American Meteorological Society, 98*(4), 737–752. https://doi.org/10.1175/BAMS-D-16-0057.1

McCarthy, G., Frajka-Williams, E., Johns, W. E., Baringer, M. O., Meinen, C. S., Bryden, H. L., et al. (2012). Observed interannual variability of the Atlantic meridional overturning circulation at 26.5°N. *Geophysical Research Letters, 39*, L19609. https://doi.org/10.1029/2012GL052933

McCarthy, G. D., Haigh, I. D., Hirschi, J., Grist, J. P., & Smeed, D. A. (2015). Ocean impact on decadal Atlantic climate variability revealed by sea-level observations. *Nature, 521*(7553), 508–510. https://doi.org/10.1038/nature14491

McCarthy, G. D., Smeed, D. A., Johns, W. E., Frajka-Williams, E., Moat, B. I., Rayner, D., et al. (2015). Measuring the Atlantic Meridional Overturning Circulation at 26 °N. *Progress in Oceanography, 130*, 91–111. https://doi.org/10.1016/j.pocean.2014.10.006

Meinen, C. S., Speich, S., Perez, R. C., Dong, S., Piola, A. R., Garzoli, S. L., et al. (2013). Temporal variability of the meridional overturning circulation at 34.5°S: Results from two pilot boundary arrays in the South Atlantic. *Journal of Geophysical Research: Oceans, 118*, 6461–6478. https://doi.org/10.1002/2013JC009228

Polo, I., Robson, J., & Sutton, R. (2014). The importance of wind and buoyancy forcing for the boundary density variations and the geostrophic component of the AMOC at 26N. *Journal of Physical Oceanography, 44*(9), 2387–2408. https://doi.org/10.1175/JPO-D-13-0264.1

Rahmstorf, S., Box, J. E., Feulner, G., Mann, M. E., Robinson, A., Rutherford, S., & Schaffernicht, E. J. (2015). Exceptional twentieth-century slowdown in Atlantic Ocean overturning circulation. *Nature Climate Change, 5*(5), 475–480. https://doi.org/10.1038/nclimate2554

Rayner, N. A., Parker, D. E., Horton, E. B., Folland, C. K., Alexander, L. V., Rowell, D. P., et al. (2003). Global analyses of sea surface temperature, sea ice, and night marine air temperature since the late nineteenth century. *Journal of Geophysical Research, 108*(D14), 4407. https://doi.org/10.1029/2002JD002670

Roberts, C. D., Garry, F. K., & Jackson, L. C. (2013). A multimodel study of sea surface temperature and subsurface density fingerprints of the Atlantic Meridional Overturning Circulation. *Journal of Climate, 26*(22), 9155–9174. https://doi.org/10.1175/JCLI-D-12-00762.1

Robson, J., Hodson, D., Hawkins, E., & Sutton, R. (2013). Atlantic overturning in decline? *Nature Geoscience, 7*(1), 2–3. https://doi.org/10.1038/ngeo2050

Smeed, D., McCarthy, G., Rayner, D., Moat, B. I., Johns, W. E., Baringer, M. O., & Meinen, C. S. (2017). *Atlantic meridional overturning circulation observed by the RAPID-MOCHA-WBTS (RAPID-Meridional Overturning Circulation and Heatflux Array-Western Boundary Time Series) array at 26N from 2004 to 2017*. UK: British Oceanographic Data Centre-Natural Environment Research Council. https://doi.org/10.5285/5acfd143-1104-7b58-e053-6c86abc0d94b

Smeed, D. A., McCarthy, G. D., Cunningham, S. A., Frajka-Williams, E., Rayner, D., Johns, W. E., et al. (2014). Observed decline of the Atlantic meridional overturning circulation 2004-2012. *Ocean Science, 10*(1), 29–38. https://doi.org/10.5194/os-10-29-2014

Thomas, M. D., de Boer, A. M., Stevens, D. P., & Johnson, H. L. (2012). Upper ocean manifestations of a reducing meridional overturning circulation. *Geophysical Research Letters, 39*, L16609. https://doi.org/10.1029/2012GL052702

Tulloch, R., & Marshall, J. (2012). Exploring mechanisms of variability and predictability of Atlantic Meridional Overturning Circulation in two coupled climate models. *Journal of Climate, 25*(12), 4067–4080. https://doi.org/10.1175/JCLI-D-11-00460.1

van Sebille, E., Baringer, M. O., Johns, W. E., Meinen, C. S., Beal, L. M., de Jong, M. F., & van Aken, H. M. (2011). Propagation pathways of classical Labrador Sea water from its source region to 26°N. *Journal of Geophysical Research, 116*, C12027. https://doi.org/10.1029/2011JC007171

Yashayaev, I., & Loder, J. W. (2016). Recurrent replenishment of Labrador Sea Water and associated decadal-scale variability. *Journal of Geophysical Research: Oceans, 121*, 8095–8114. https://doi.org/10.1002/2016JC012046

Zhang, R. (2008). Coherent surface-subsurface fingerprint of the Atlantic meridional overturning circulation. *Geophysical Research Letters, 35*, L20705. https://doi.org/10.1029/2008GL035463

Zhao, J., & Johns, W. (2014a). Wind-driven seasonal cycle of the Atlantic Meridional Overturning Circulation. *Journal of Physical Oceangraphy, 44*(6), 1541–1562. https://doi.org/10.1175/JPO-D-13-0144.1

Zhao, J., & Johns, W. (2014b). Wind-forced interannual variability of the Atlantic meridional overturning circulation at 26.5°N. *Journal of Geophysical Research: Oceans, 119*(4), 2403–2419. https://doi.org/10.1002/2013JC009407